Saccadic lens instability increases with accommodative stimulus in presbyopes

Lin He — College of Optometry, University of Houston, Houston, TX, USA

William J. Donnelly III — Breault Research Organization, Tucson, AZ, USA

Scott B. Stevenson — College of Optometry, University of Houston, Houston, TX, USA

Adrian Glasser — College of Optometry, University of Houston, Houston, TX, USA

An SRI dual Purkinje image (dPi) eye tracker was used to measure lens wobble following saccades with increasing accommodative effort as an indirect measure of ciliary muscle function in presbyopes. Ten presbyopic subjects executed 32 four-degree saccades at 1-s intervals between targets arranged in a cross on illuminated cards at each of 9 viewing distances ranging from 0.5- to 8-D accommodative demands. Post-saccadic lens wobble artifacts were extracted by subtraction of P1 (H_1/V_1) position signals from P4 signals (θ_H/θ_V), both of which were sampled by the eye tracker at 100 Hz. A ray tracing eye model was also employed to model the fourth Purkinje image shifts for a range of lens translations and tilts. Combining all saccades from all subjects showed a significant positive relationship between lens wobble artifact amplitude and accommodative demand. Eye model simulations indicated that artifacts of the amplitude measured could arise from either lens tilts (in the range of 2–4 degrees) or lens translations (in the range of 0.1 to 0.2 mm). Saccadic lens wobble artifacts increase with accommodative effort in presbyopes, indicating preserved ciliary muscle function and greater relaxation of zonular tension with accommodative effort. Variation across subjects may reflect differences in accommodative effort, ciliary muscle function for a given effort, and/or in intraocular anatomy.

Introduction

The etiology of presbyopia remains unclear. Presbyopia could occur consequent to loss of ciliary muscle function or loss of lens function. Several studies suggest loss of lens compliance as the primary pathology (Glasser & Campbell, 1998, 1999; Heys, Cram, & Truscott, 2004; Weeber et al., 2005; Weeber, Eckert, Pechhold, & van der Heijde, 2007; Weeber & van der Heijde, 2008). Current approaches aimed at restoration of accommodation in presbyopes with accommodating lens implants assume that ciliary muscle function is preserved in the aging eye. Continued ciliary muscle function is of course imperative if accommodation is to be restored. The extent to which ciliary muscle function contributes to presbyopia has been debated. Two competitive theories exist. Gullstrand (1908) and Hess (1901) suggested that the ciliary muscle could retain most of its contractile function with age and that loss of ciliary muscle function contributes little to the progression of presbyopia. On the other hand, Duane

(1912, 1922) and Fincham (1937, 1955) considered that gradual loss of ciliary muscle contraction should also be considered as a cause of presbyopia in addition to age-related changes in the lens. Refractometers can be used to measure the accommodative optical change in power of the eye. However, since lens stiffness increases with age (Heys et al., 2004; Weeber et al., 2005, 2007; Weeber & van der Heijde, 2008), the lens is ultimately unable to change shape during accommodation in the presbyopic eye (Glasser & Campbell, 1998; Strenk et al., 1999). Thus refractive measurements cannot be used to evaluate ciliary muscle function. New technologies have been applied to address the problem. Magnetic resonance imaging (MRI; Strenk et al., 1999; Strenk, Stenk, & Guo, 2006) and ultrasound biomicroscopy (UBM; Stachs et al., 2002) have been used to evaluate ciliary muscle function through biometric measurements. Studies using both techniques conclude that ciliary muscle accommodative movements are preserved even in the presbyopic eye.

The ciliary muscle, zonular fibers, lens capsule, and lens substance function as an accommodative unit. If the

accommodative function of one of these structures is reduced, accommodative amplitude would be limited. In this study, a dual Purkinje image (dPi) eye tracker was used to evaluate the extent to which the ciliary muscle/ zonular complex responds during accommodation in presbyopes. Unlike the imaging techniques mentioned above, the dPi eye tracker can do dynamic measurement at temporal frequency of 100 Hz or more. The dPi eye tracker is a non-contact optical instrument and is unobtrusive and easy to use because it does not require an eye coil or a saline bath on the eye.

The dPi eye tracker was developed to measure eye movements and accommodative changes in the lens (Cornsweet & Crane, 1973; Crane & Steele, 1985). The use of the dPi eye tracker to monitor lens movements within the eye was first reported by Crane and Steele (1978) when they improved the design of the eye tracker. They noticed that the eye tracker could record lens oscillatory "overshoots" during tracking of the saccadic eye movements of most subjects and the size of the overshoots varied with the level of accommodation. They attributed the overshoots to a lateral motion of the lens within the eye (Crane & Steele, 1978). In addition to lens motion artifacts, overshoots recorded by the eye tracker may include three different saccadic characteristics found in dynamic recordings that have been called dynamic overshoot, glissade, and static overshoot (Bahill, Clark, & Stark, 1975a, 1975b; Kapoula, Robinson, & Hain, 1986). The overshoot recorded by the dPi eye tracker appears similar to a "dynamic overshoot", which can be recorded either with a pair of photodiodes (Bahill et al., 1975b) or magnetic field search coil (Kapoula et al., 1986). The dynamic overshoot occurs at the end of a saccade when the eye movement exceeds its intended position and then corrects in the opposite direction with large velocities on the order of 10–100 deg/s. If eye tracker recorded overshoots are dynamic overshoots, this means they are of ocular saccadic origin and are not relevant to lens motion. Deubel and Bridgeman (1995) attempted to record saccades in the relaxed and accommodated states of 11 subjects, 20–56 years old, by using both a dPi eye tracker and an eye coil. Since the eye coil records only eye rotation and not lens movements, the authors subtracted the eye coil recorded profiles from corresponding dPi eye tracker recorded profiles. In this way, they justified that the subtracted profiles were due to pure lens deviations. Therefore, they concluded that the overshoots recorded by the dPi eye tracker originated from lens deviations within the eye. Moreover, they found that these overshoots were larger when the eye was accommodated. Saccades produce large accelerations and decelerations of the eye as well as motion of the lens within the eye. Since the lens is suspended by the zonular fibers in the eye, the lens can have a range of relative motion with respect to the eye due to inertia in specific conditions such as following saccades. Because the dPi eye tracker tracks the P4 reflection from the posterior lens surface, it should be able to measure the relative motion of lens within the eye. Since the precise source of the overshoot is uncertain (discussed below), in this study the overshoot is referred to as "lens wobble artifact".

Testing was performed in ten fully presbyopic subjects and one 49-year-old subject who still had 1.34 D of objectively measured accommodative response. Subjects were required to make controlled saccades to visual stimuli presented at various vergence demands. Continuous, dynamic Purkinje image recordings were made with the eye tracker. The amplitude of the lens wobble artifacts at different accommodative stimulus demands was used to quantify their relationship. High-speed video recordings of lens wobble were also analyzed during saccades in the unaccommodated and accommodated states of one individual with a small cataract. A ray tracing eye model (Advanced Human Eye Model, AHEM, Breault Research Organization) was also employed to model P4 shifts caused by a range of translations and tilts of the lens within the eye.

Methods

Subjects

The research was performed in accordance with an institutionally approved human subjects protocol with informed consent and followed the tenets of the Declaration of Helsinki.

Ten human subjects aged from 53 to 71 (mean = 61.0, SD = 6.0), including six males and four females, were recruited from the College of Optometry. Exclusion criteria were given as follows:

1. Incomplete presbyopes (individuals with objectively measurable accommodative amplitude greater than 0.5 D);
2. Subjects with ocular disease involving the lens or iris, or eye movement abnormalities;
3. Subjects who had had cataract surgery in either eye;
4. Subjects with astigmatism greater than ±1.50 D.

Refractive errors ranged from +1.25 D to −4.50 D, with a mean (±SE) of −1.30 ± 1.91 D. Astigmatism ranged from −0.50 D to −1.50 D, with a mean (±SE) of −0.58 ± 0.59 D. The spherical equivalent refractive errors were corrected to within ±0.25 D by soft contact lenses in both eyes during accommodation measurements and eye tracker recordings. Accommodation was measured with an autorefractor (WR-5100K, Grand Seiko) to exclude incomplete presbyopes who had more than 0.50 D of objectively measurable accommodation. Subjects were asked to fixate on a distant letter chart at 6 m and then on near letter charts pushed up to 16.7 cm (corresponding

to accommodative stimuli of 0 to 6.0 D with incremental steps of 1.0 D). Subjects were asked to focus on the letters binocularly. For each target distance, three measurements were recorded by the autorefractor in the left eye. All subjects tested had accommodative responses less than 0.50 D. One subject was excluded due to having had prior cataract surgery with intraocular lens implantation in her left eye. Ten full presbyopic subjects participated in the study. These subjects had between +0.07 D to 0.50 D of accommodation, with a mean ± SD of −0.29 ± 0.15 D.

The experiment was also performed in another subject, 49 years of age, with a refractive error of −0.50 D and astigmatism of −1.25 D with 1.34 D of accommodation. This subject was included to compare lens wobble artifact amplitudes before and after cycloplegia in addition to one of the presbyopic subjects included above. All eye examinations and applications of eye drops were performed by a licensed clinician from the College of Optometry.

High-speed lens wobble video recordings

The 49-year-old subject with a 1.34-D accommodative response had a small, focal, off-axis cuneiform cataract. The cataract was readily visible in the dilated eye in a video image with high magnification and infrared retro-illumination (Movie 1). Video-based tracking of the cataract using a 60-Hz frame rate infrared sensitive
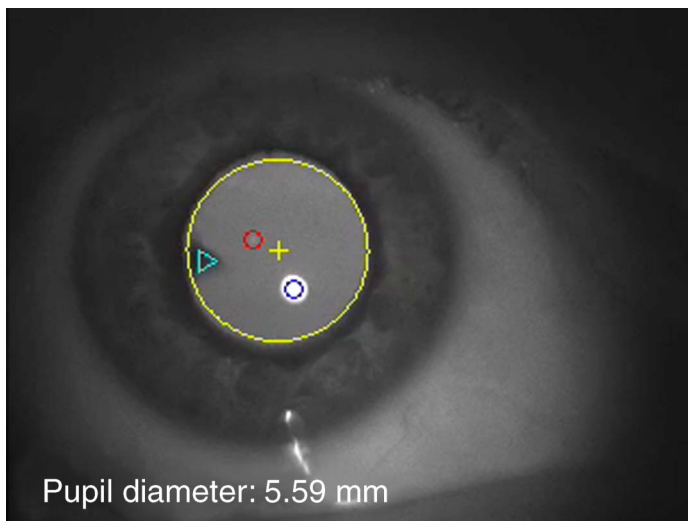
Movie 1. A video clip that was captured from an incomplete presbyope who still retained 1.34 D of accommodation. The large yellow circle marks the pupil edge and the yellow cross marks the center of the pupil. The small blue and red circles marked P1 and P4, respectively. The triangle marks the cuneiform cataract in the lens. Notice that the initial pupil diameter was above 7 mm and when the subject started to accommodate during saccades, the pupil diameter decreased below 5 mm. As the subject accommodates, the lens wobble becomes be more pronounced.

charge-coupled device (CCD) camera (Basler AG, A311f) provided a video method to record lens wobble directly in this subject. Similar methods have been reported to image and analyze P1 and P4 to estimate "crystalline lens tension" (Schultz, Sinnott, Mutti, & Bailey, 2009). In the current study, P1, P4, and the focal cuneiform cataract were all visible within the dilated pupil so that video image analysis could be performed and the relative movement of the lens could be calculated using the same algorithm comparing relative movements of P1 and P4 and the cataract as used with the eye tracker. Since the position of the cataract was fixed with respect to the lens, the tracked cataract image position could then be considered as a reference to evaluate the reliability of using P1 and P4 to track the lens motion. A custom Matlab program was used to find the pupil margin and center, the focal cataract, P4, and P1 in each frame of the video. Accuracy was checked by marking these features in each frame with a symbol (Movie 1). Relative P4 and cataract movements with respect to P1 were obtained by subtracting P4 and cataract positions from the P1 position. These two relative traces during saccades were compared by a correlation analysis to validate the use of the eye tracker's relative P4 to represent the relative lens motion during saccades.

Measurement of lens wobble artifact

Recordings were made with the Generation V Dual Purkinje Image (dPi) eye tracker (SRI International; Cornsweet & Crane, 1973; Crane & Steele, 1985) with Microsoft Visual Basic code. The subjects sat in the eye tracker, with their heads positioned in a chin cup. A bite bar was used with 2 subjects for better fixation but could not be used in all subjects due to dental constraints. Viewing was binocular and left eye position and movements were monitored by the dPi eye tracker from its θ_H/θ_V and H_1/V_1 channels. The computer acquired the digital signals at 360 Hz from these four channels via an analog-to-digital (A/D) converter. Two drops of phenyl-ephrine were applied to the left eye of all subjects to provide large enough pupil diameters to facilitate the eye tracker P4 recordings. Testing was performed in the dilated eye of the 49-year-old subject and in one full presbyope once without and on another occasion after two drops of tropicamide administered to paralyze accommodation. The visual stimuli consisted of five printed black Snellen "E" letters arranged on illuminated cards, one each above, below, left, and right of a central letter. Each set of five letters served as the saccadic and accommodative stimuli. Stimuli were placed at 9 viewing distances for accommodative demands of 0.5 D, 1 D, 2 D, 3 D, 4 D, 5 D, 6 D, 7 D, and 8 D. At each viewing distance, each letter was separated from the center letter by four degrees. Letters were 5 mm in size (corresponding to Snellen sizes of 20/60) for the 200-cm viewing distance and 2.5 mm in

size for all other distances (corresponding to 20/69, 20/138, 20/206, 20/275, 20/344, 20/413, 20/481, 20/550).

The stimuli were viewed binocularly all the time. Subjects were initially aligned in the eye tracker with the letter stimulus chart at each test distance aligned with the left eye in primary gaze, and as a result, only the right eye underwent a convergent change when the nearer stimulus was viewed. The subjects were instructed to make an effort to focus on the letters as clearly as possible during testing. Although all subjects but one were presbyopic and could not accommodate, the stimuli were intended to get subjects to exert a voluntary ciliary muscle contraction. Purkinje image recordings were made continuously as subjects executed a total of 32 four-degree saccades at 1-s intervals by following timed, computer-generated auditory instructions in a fixed order, repeated three times. The target luminance was measured to be between 50 and 100 cd/m^2 by a Minolta LS-110 Luminance Meter (Konica Minolta Sensing).

The eye tracker projects a 930-nm collimated infrared light from an extended source into the left eye and tracks P1 reflected from the anterior surface of the cornea and P4 reflected from the posterior surface of the lens by its H_1/V_1 and θ_H/θ_V channels, respectively. In this way, coupled movement of P1 and P4 indicates head movement while differential movement between the two Purkinje images indicates eye rotation. The H_1/V_1 channel represents the angular position of P1 while the θ_H/θ_V channel represents the difference in angular position between P1 and P4. Both θ_H/θ_V and H_1/V_1 channels were converted from voltage signals into angular position signals in degrees. All subjects were assumed to fixate accurately. The task subjects were asked to perform, i.e., making 4° saccades to sequentially fixate an array of targets, was the same as the general method used to calibrate the dPi eye tracker. Therefore, fixation targets in the study also served as a calibration for the angular extent of eye movement recorded by the eye tracker.

The bandwidth of the eye tracker was measured with a galvanometer driven, artificial eye. The artificial eye has two glass reflective surfaces designed with curvatures similar to the anterior cornea surface and posterior lens surface and at similar positions as in a human eye. The artificial eye also has a rear plano mirror that can be used to calibrate the angular movement of the artificial eye. The frequency of the rotation of the artificial eye was gradually increased until the rotational amplitude recorded by the eye tracker dropped to half, which implied a gain loss of 3 dB and provided the bandwidth of the eye tracker. The eye tracker was found to have a bandwidth of around 100 Hz. Therefore, as long as the lens oscillation has a frequency of less than 50 Hz, it can be detected by the eye tracker without loss of signal amplitude.

As previous studies have shown, brief artifacts are recorded from the θ_H/θ_V channel at the end of saccades (Crane & Steele, 1978; Deubel & Bridgeman, 1995). The origin of these artifacts is assumed to be from relative
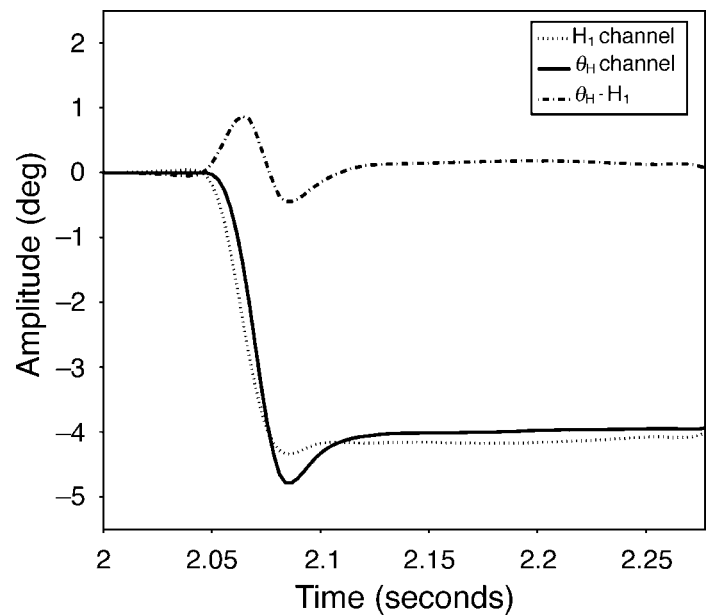

Figure 1. Recordings from a four-degree, leftward saccade to a 0.5-D accommodative stimulus. The output signals from the H_1 channel (P1: dotted line) and the θ_H channel (P4–P1: solid line) are shown. Subtracting H_1 from θ_H shows the lens wobble artifact (dash-dot line) that is assumed to represent the wobble of the lens within the eye.

lateral motion of the lens within the globe although lens tilt may also contribute. Figure 1 shows typical recorded positional signals from the H_1 channel (dotted line) and the θ_H channel (solid line) before, during, and after a saccade. There is a time lag of θ_H relative to H_1 of about 4–8 ms. This lag could be due either to the asynchronous eye-lens motion as Crane and Steele (1978) first described, or to a system error of the eye tracker itself. The artificial mechanical eye with a "cornea" surface and a fixed and immovable "lens" surface was used to check the latency when driven by the servomotor with a 4-degree step movement. In the model eye, the relative θ_H lag was less than 2 ms. In general, the model eye latency is less than 20% of that in the real eye. Therefore, the relative lag observed with natural eyes is likely to reflect "backshoot" of the lens as described by Deubel and Bridgeman (1995).

Videographic pupillography

A video camera (Cohu, Model 4912-2000) with an array of infrared LEDs on axis in front of the camera lens was also used simultaneously during the eye tracker measurement to record right eye convergence responses and pupil diameters in all subjects to ensure that subjects were making an effort to accommodate on the near target. The recorded video from one subject was analyzed to determine the relationship between convergence response and pupil size. Pupil center and the pupil size were

Parameter	Value
IR wavelength	930 nm
Eye lens model	Biconvex
Field angle	−33.0 deg
AZ accommodative lens power	0 D
Lens anterior vertex position	2.970 mm
Lens center thickness	3.767 mm
Lens diameter	10.00 mm
Lens anterior radius of curvature (and conic constant)	12.000 mm (−7.519)
Lens posterior radius of curvature (and conic constant)	−5.225 mm (−1.354)
Lens refractive index	1.42
Cornea center thickness	0.550 mm
Cornea anterior radius of curvature (and conic constant)	7.800 mm (−0.250)
Cornea posterior radius of curvature (and conic constant)	6.500 mm (−0.250)
Cornea diameter	12.00 mm

Table 1. Parameters in AHEM to simulate P4 image shifts for a range of lens translations and tilts.

measured first when the subjects were asked to focus on the center letter "E", and then compared with those from other image frames during accommodation and during saccades. Video clips were analyzed from when the subject was fixated at far and near to compare simultaneous videographically measured pupil diameters and saccadic eye movements.

Ray tracing eye model

A ray tracing eye model (Advanced Human Eye Model, AHEM, Breault Research Organization) was used to model the fourth Purkinje image shifts for a certain range of lens translations and tilts within the eye. AHEM is used with ASAP optical engineering software to model light propagation inclusive of refraction, diffraction, and scattering (Donnelly, 2008). It is a binocular eye modeling system that can be integrated and exported with other opto-mechanical systems. The parameters adopted by AHEM are based on the AZ Accommodative Eye Model (Schwiegerling, 2004). The eye model parameters used are detailed in Table 1.

Data analysis

Exclusion of saccadic component

P1, the reflection from the anterior corneal surface, will move with either rotational or translational eye movement. The eye movements of interest to this study are rotational eye movement. Translational eye movements relative to the eye tracker can also occur but are primarily the result of head movements. P4 is the reflection from the posterior surface of the lens. Apart from rotation and translation that cause movements of P1 and P4, the artifact found in the difference between the P1 and P4 signals is caused by relative crystalline lens movement. The dPi eye tracker subtracts P1 from P4 and generates a signal sent out from its θ_H/θ_V channel to represent eye rotation without translation artifacts. However, this signal also includes lens wobble effects. Subtraction of the P1 movement from the θ_H/θ_V signal thus provides a signal primarily reflecting the lens wobble artifact.

To verify that the artifacts come from relative crystalline lens deviations rather than from saccades directly, amplitudes of H_1/V_1 and θ_H/θ_V were calibrated and matched with each other by using custom Matlab code. θ_H/θ_V and H_1/V_1 were plotted with respect to each other and fitted with a linear regression with a zero intercept. The slope of this linear regression was then used to adjust the H_1/V_1 amplitudes to match the θ_H/θ_V amplitudes. This procedure matched the gain of H_1/V_1 and θ_H/θ_V channels with respect to eye rotation, so that they could be subtracted from each other. Subtracting the scaled H_1/V_1 signal from the θ_H/θ_V signal excludes the saccadic component of the recorded signals and shows a lens deviation artifact if it exists. The dash-dot line shown in Figure 1 is the result after this matching and subtraction is applied.

Frequency analysis

The analysis described above could include a head movement even though the saccadic eye movement is excluded. To ensure that the artifact does not originate from a head movement, subtracted profiles during saccades were compared with those from segments immediately preceding saccades. This analysis assumes that if a head movement was occurring immediately preceding a saccade, it would have continued during the saccade as well. The interval between the compared profiles was around 10 ms and the profiles were 280 ms in length. A fast Fourier transform (FFT) was applied to convert the difference profiles from before and during the saccades into the frequency domain using custom written Matlab code. A Hamming window was used to filter low frequency drifts in the subtracted profiles, mainly between 0 and 3.57 Hz. The frequency of head movement should be relatively low (0.5–5.0 Hz, Melvill Jones & Gonshor, 1982) compared with lens wobble, which is around 20 Hz. If head movements are occurring, the assumption is that artifacts caused by head movements would occur with a fixed low frequency range between 3.57 and 5.0 Hz in the recordings preceding and during the saccades in the Fourier domain. If head movement was the only component in both recordings, the peaks in the amplitude spectra corresponding to head movements should appear at similar frequencies in both recordings and no other obvious peaks should be observed during saccades.

Otherwise, a relatively high frequency peak that indicates crystalline lens deviations should be evident but only in the recordings during the saccades, not in the recordings before the saccades.

Artifact and accommodation

The peak-to-trough distance in the subtracted profiles as shown in Figure 1 was used to calculate the amplitude of each artifact. Although subjects were asked to make 4-degree saccades, the actual saccade amplitude varied across subjects and conditions. Comparison of artifact amplitude to saccade amplitude over all subjects showed a positive correlation (see Results section). In order to exclude the effect of saccade amplitude from the analysis, the ratio of artifact amplitude to saccade amplitude was calculated. This artifact/saccade ratio was then compared with the accommodative stimulus amplitude to determine whether the lens would become less stable with the increase in accommodative stimulus. After a linear regression was performed, a significance test for regression slope was applied based on the null hypothesis that the regression slope is equal to zero, i.e., artifact amplitude does not depend on accommodative stimulus amplitude. The statistics test was performed with MINITAB (Minitab).

Results

Lens wobble artifacts

The 60-Hz movies captured from the 49-year-old subject with a cataract demonstrated the saccadic lens wobble, which is especially evident when the subject makes an accommodative effort (Movie 1). The video clip was recorded when the subject was fixating on a distant target while making saccades and then while accommodating on a near target and making saccades. Figure 2A shows data recorded from three saccades, two upward and one downward, from about 2 s of the video during accommodative effort. Neither the pupil center coordinates nor the P1 coordinates were associated with lens wobble. However, both P4 and cataract traces were associated with lens wobbles during the saccades. The correlation between the P4 wobble and cataract wobble during saccades shows these two traces were well correlated in general (Figure 2B), which means that P4 can be used as a reliable indicator of lens motion. The videographically recorded data were analyzed in essentially the same way as the eye tracker data to compare the relative movements of P1 and P4 as a measure of lens wobble. The presence of the cataract in the videographic data therefore demonstrates that this analysis provides a reliable way to measure lens wobble.

Phenylephrine was used to dilate the pupil, and pupil constriction still occurred when the subject attempted to accommodate. Accommodative effort caused the lens to be under reduced zonular tension and to wobble during saccades. Lens wobble artifacts determined by subtraction of the Purkinje images with the dPi eye tracker were plotted as in Figure 3, which shows data from one subject. The form of the artifact is relatively consistent, especially at lower accommodative stimulus amplitudes. The profiles are typically biphasic in shape. Since the saccadic component has been excluded in the subtracted profiles and lens deviation was clearly visible in the videos, the lens wobble artifact is not a recording of the saccade.
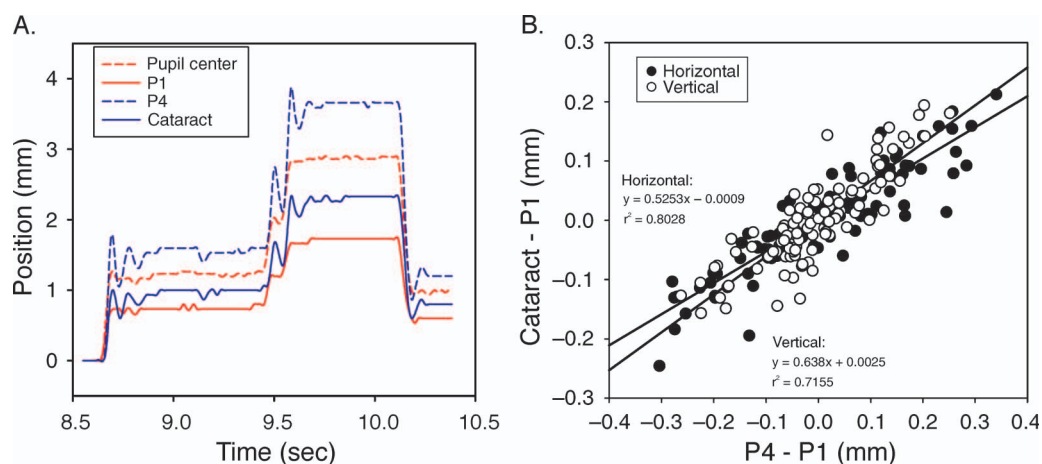

Figure 2. (A) Three vertical saccades recorded by a high-speed video camera. The red lines are traces from the pupil center (dashed line) and from P1 (solid line) and are not associated with the lens. The blue lines are traces from P4 (dashed line) and the cataract (solid line) and are associated with the lens. These lines are vertically offset with respect to each other so they can be distinguished. (B) A correlation between cataract wobble and P4 wobble from 12 vertical saccades in a video clip. A good correlation is observed for both the horizontal and vertical relative movements and the slope of the regressions were similar.
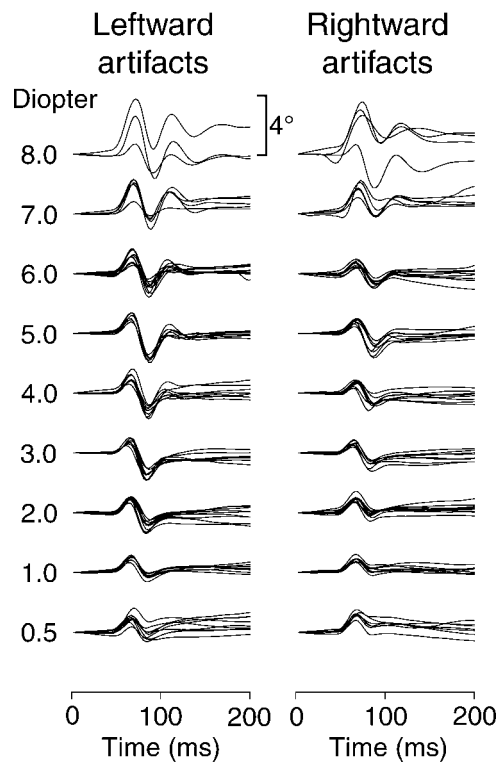
Figure 3. The lens wobble artifacts as a function of time for nine accommodative stimuli during horizontal saccades from one subject (HEB). The 4° scale applies to all recordings. Lens wobble amplitude increases with accommodative stimulus demand.

A fast Fourier transform of the subtracted profiles before saccades and during saccades provided information on the frequency content of the responses. Figure 4 presents the results from one of the noisier subjects in terms of head movement. As expected, the curves coincide at low frequencies indicating that head movements are present in the recordings both preceding and during the saccades. The first part of each recording shows a "peak" corresponding to the head movement. The recordings during, but not those from before, saccades showed an additional peak frequency at $e^{3.0} = 20.1$ Hz, corresponding to the lens wobble. This demonstrates that the post-saccadic recordings contained a lens wobble artifact of a higher frequency component than head movements.

Convergence and pupil size

To maximize accommodative effort made by the presbyopes, a system was set up to take advantage of as many accommodative cues as possible. The target was moved closer to the subjects to provide blur and proximal cues and the task was performed binocularly to provide convergence cues. The convergence response was measured with

infrared videographic pupillography and analysis from one subject shows that the calculated convergence in prism diopters was significantly correlated with the accommodative stimulus amplitudes ($r^2 = 0.958$, $F[1, 17] = 389.89$, $p < 0.001$; data not shown). All subjects viewed binocularly but maintained single vision for the different accommodative stimuli. The convergence was therefore proportional to the stimulus amplitudes.

Pupil diameter also gives some indication of accommodative effort since the pupils constrict during accommodation. Video analysis in one subject also shows that the pupil diameter decreased linearly with the accommodative stimulus ($r^2 = 0.887$, $F[1, 17] = 133.50$, $p < 0.001$; data not shown). Pupil diameters were also videographically analyzed from immediately preceding the saccades. The near reflex includes accommodation and pupil constriction. If the subject did make accommodative efforts, the pupil might serve as an indicator of how much accommodative efforts the subject made. Therefore, the pupil diameters were compared with the artifact amplitudes from the same saccade. The result showed no correlation between pupil diameter and the lens wobble artifact amplitudes, both for low accommodative demands (e.g., 0.5 D: $r^2 = 0.030$, $F[1, 30] = 0.92$, $p = 0.346$) and for
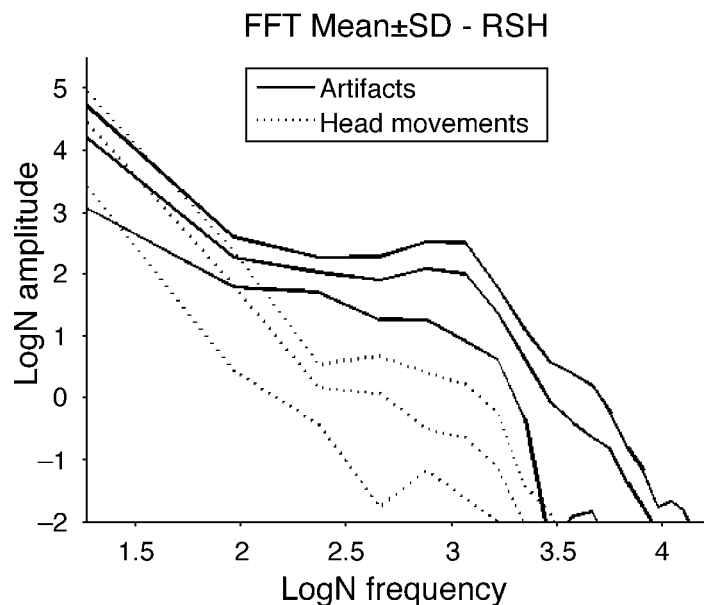

Figure 4. The amplitude spectra by fast Fourier transform in natural logarithmic scale from one of the noisier subjects in terms of head movement. Each trace is from a single 280-ms record segment after subtracting H$_1$ from θ_H, which isolates lens wobble but also may include head motion. The dashed lines are from sections immediately preceding saccades and the solid lines are from the same recordings during saccades. There is no obvious peak in the recordings preceding saccades while the recordings during saccades have peaks around $e^{3.0} = 20.1$ Hz, indicative of the lens wobble artifacts.
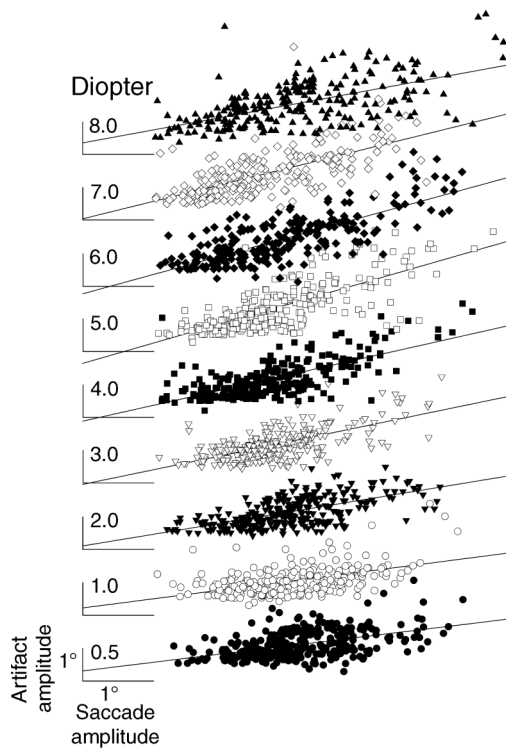
Figure 5. Artifact amplitude (in degrees) plotted as a function of the saccade amplitude for different accommodative stimuli (in diopters) from all the subjects. All the linear regressions shown are statistically significant at the $p < 0.001$ level as shown in Table 2. Degree scale on the lowest trace applies to all.

high accommodative demands (e.g., 5.0 D: $r^2 = 0.054$, $F[1, 30] = 1.72$, $p = 0.200$).

Artifact amplitude and artifact/saccade ratio

When the relationship between artifact amplitude and accommodative stimulus was investigated, larger saccades tended to give larger artifacts. Collewijn, Erkelens, and Steinman (1988a, 1988b) showed that larger saccades had larger peak velocities and accelerations. Larger accelerations imply that larger forces are exerted. Because the forces causing saccades are the same forces that would cause the lens to wobble, it would be expected that saccade amplitudes affect artifact amplitudes. To test this assumption, artifact amplitude was plotted as a function of saccade amplitude within each accommodative stimulus demand. A linear regression was fit to each artifact amplitude versus saccade amplitude graph (Figure 5). The recorded saccade amplitudes were between 1 and 6 degrees and artifact amplitude increased with saccadic amplitude. The regression slopes, their respective correlation coefficients, and p-values for different accommodative stimulus demands are listed in Table 2. The regression slopes and coefficients increase with increasing

stimulus demand to 6 D and then decrease. Therefore, to understand the effect of the stimulus demand rather than saccade amplitude on the lens wobble artifact, the ratio of artifact amplitude to saccade amplitude was employed. The peak velocity and saccade amplitude showed reasonable correlations similar to previous studies (e.g., Kapoula et al., 1986). Lens wobble amplitude was also analyzed as a function peak velocity. However, our measure of peak velocity is contaminated by the lens wobble artifact in the θ_H/θ_V signals and by head motion in the H_1/V_1 signals. Saccade amplitude estimates are much more reliable in our data, and since these are closely related to saccade peak velocity through the main sequence relationship, they serve as a reasonable substitute for peak velocity. Therefore, in the current study, the ratio of artifact amplitude to saccade amplitude, rather than saccadic velocity, was chosen to describe lens wobble effect.

Figure 6 is plotted from leftward saccades in all subjects. Only the leftward saccades were included so as to exclude direction as a confounding factor. Subjects are arranged in terms of the slope of this relationship with the uppermost subject having the largest slope. A linear fit was chosen so as to be able to compare the results from different subjects. Linear regression fits show that in 9/10 subjects, the ratio increases significantly ($p < 0.01$) with accommodative stimulus amplitude. However, the inter-individual difference is obvious as well. The ratio in one subject did not change with accommodative stimulus.

All the data from leftward saccades were considered together and the relative artifact/saccade ratio was calculated. The relative artifact/saccade ratio was calculated as the relative value of artifact/saccade ratio at each accommodative stimulus with respect to the average ratio at 0.5 D for each subject. The relative ratio excludes the inter-individual variation caused by different lens

Accommodative stimulus (D)	b_1	r^2	F	p-value
0.5	0.2632	0.216	83.48	<0.001
1	0.2776	0.2316	76.57	<0.001
2	0.3534	0.3775	172.22	<0.001
3	0.4457	0.4262	192.37	<0.001
4	0.4834	0.485	249.55	<0.001
5	0.6204	0.5287	288.34	<0.001
6	0.5902	0.5886	357.72	<0.001
7	0.533	0.4458	181.81	<0.001
8	0.3962	0.3872	165.55	<0.001

Table 2. Slopes (b_1) and r^2 values for the linear regression lines fit to the lens wobble artifacts as a function of saccade amplitude from the different accommodative stimuli calculated from the results in Figure 4. For all accommodative stimulus amplitudes, the lens wobble artifact amplitude increased significantly with increasing saccadic amplitude.
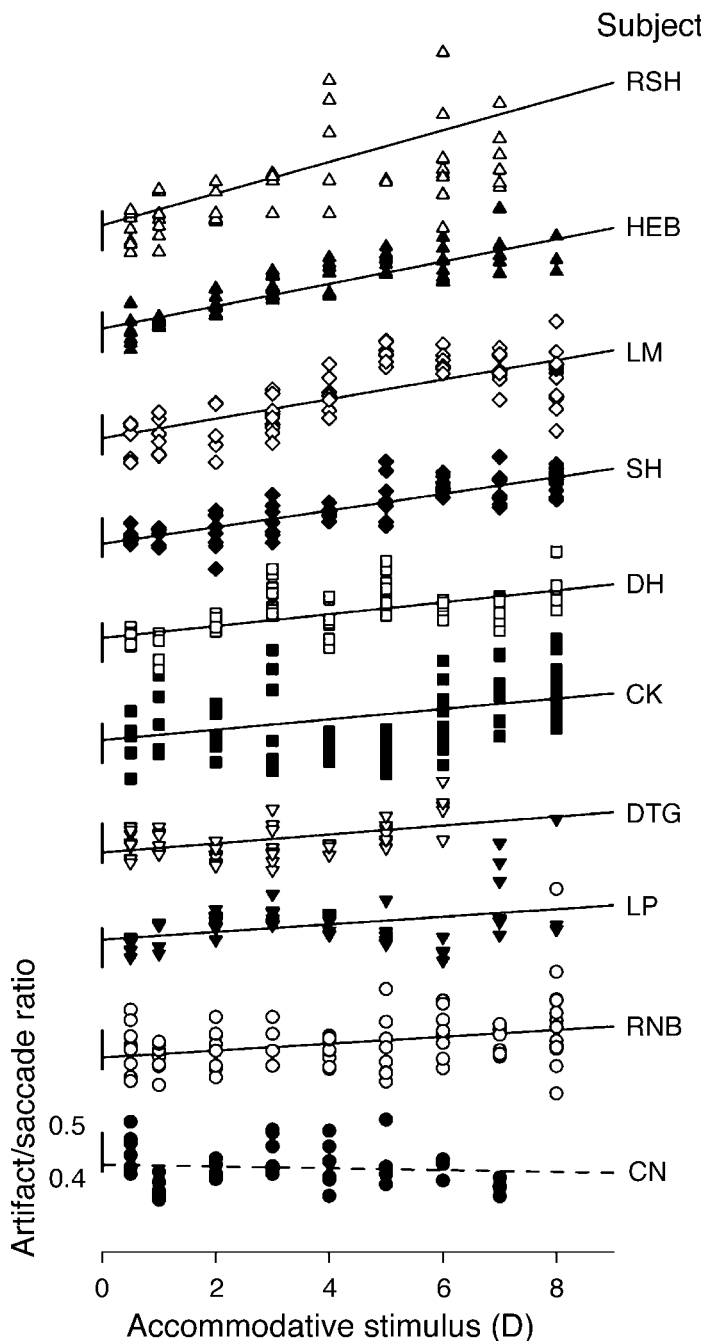
Figure 6. The ratio of artifact amplitudes to saccade amplitude was calculated and plotted as a function of 9 different accommodative stimuli. Data shown are from all leftward saccades from ten subjects. The scale bar shows a ratio of 0.5, which means the artifact amplitude is half the size of saccade amplitude. Linear regression fits show that in 9/10 subjects (all except CN), the ratio increases significantly ($p < 0.01$) with accommodative stimulus amplitude.

instabilities in each subject at the baseline level (0.5 D). A linear regression was applied to all of these leftward saccades to give a slope of 0.034. An ANOVA F-test for regression was used to test the hypothesis that the slope equaled zero. This revealed a statistical significant relationship between the artifact/saccade ratio amplitude and the accommodative stimulus amplitude ($F[1, 649] = 146.49$, $p < 0.001$; Figure 7).

Directional asymmetry

In the experiment, pairs of either horizontal (left–right or right–left) or vertical (up–down or down–up) saccades were produced. The calculated artifact amplitudes in both pairs of saccades were asymmetrical, especially the horizontal pair. The leftward saccades caused significantly larger wobble artifacts than the rightward saccades [$F(1,131) = 20.21$, $p < 0.001$; Figure 8]. Although the slope was similar, the leftward saccades had a larger intercept, indicating the asymmetry exists in the unaccommodated eye but the rate of change with accommodative stimulus demand is similar. The left eyes were tracked in all subjects, so leftward saccades were abducting saccades. Deubel and Bridgeman (1995) showed that overshoots
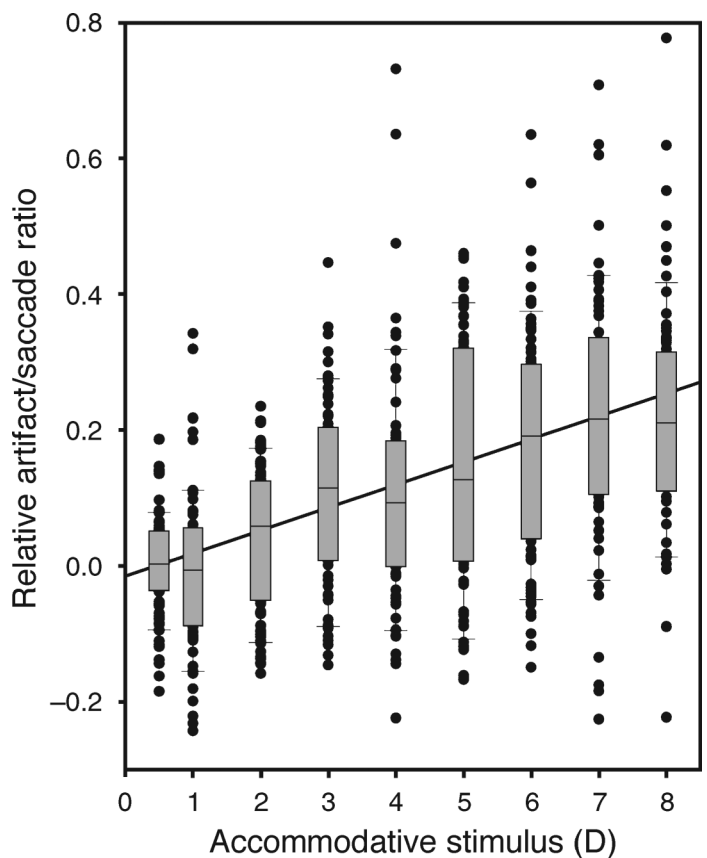

Figure 7. To better present the ratios of leftward artifact/saccade amplitude from all the subjects on the same scale, each subject's average ratio for the 0.5-D accommodative stimulus was subtracted from the ratios for all stimuli for that subject. There is a significant increase in the ratio as a function of the accommodative stimulus amplitude. Slope = 0.034 and $r^2 = 0.169$ [$F(1, 649) = 146.49$, $p < 0.001$].
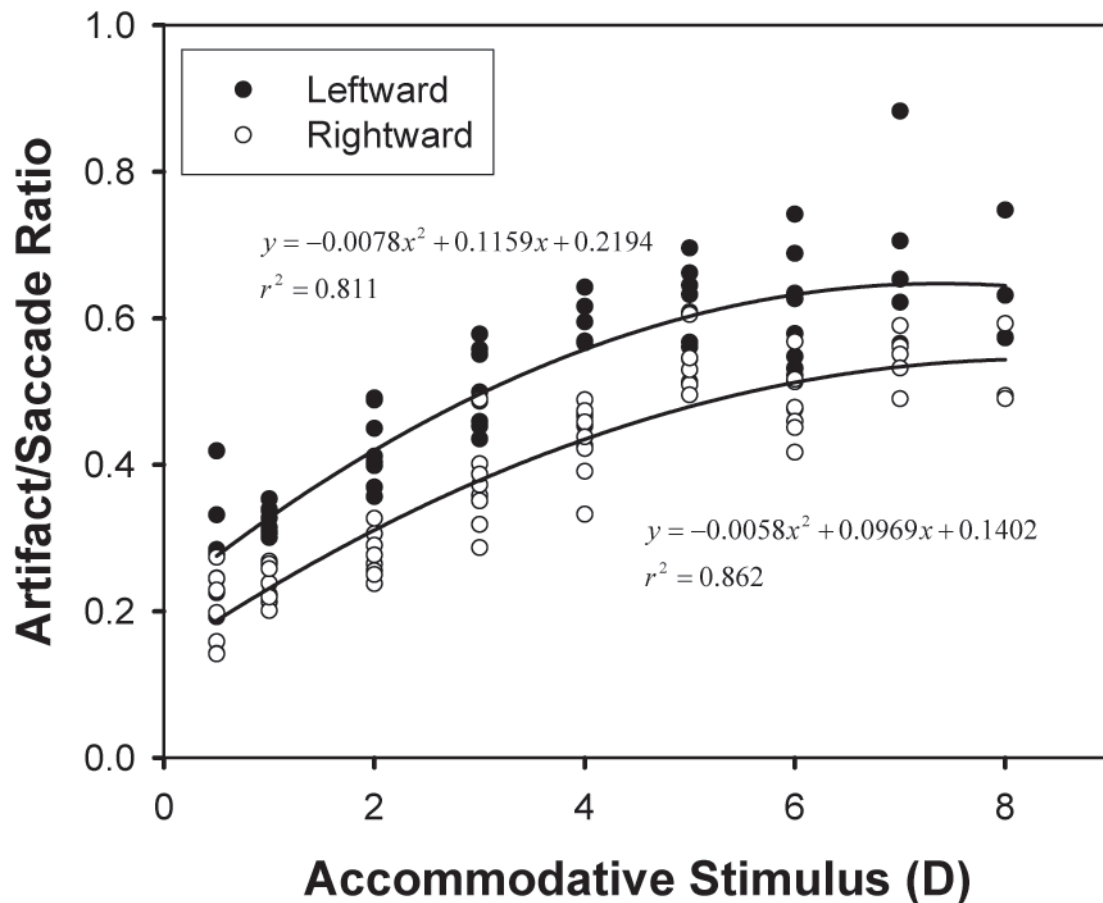
Figure 8. The artifact/saccade ratio as a function of accommodative stimulus from one subject. Two-way ANOVA shows that leftward (abducting) ratios are statistically different from rightward (adducting) ratios [$F(1, 131) = 20.21$, $p < 0.001$]. Specifically, the regression slopes are similar [$t(128) = 0.783$, $p = 0.435$], but the leftward saccades have a larger intercept [$t(128) = 7.11$, $p < 0.001$].

were significantly larger in abducting saccades than in adducting saccades.

Purkinje image tracking was performed in the right eye of one subject to see whether the directional asymmetry also occurred in the right eye. The results showed that abducting (rightward) saccades had larger artifact amplitudes, which indicated that the directional asymmetry was mirror symmetrical. Collewijn et al. (1988a) studied the relationship of saccade amplitude and peak velocity between these two opposite horizontal directions and found that abducting saccades always had larger saccade amplitudes and peak velocities. The θ_H/θ_V and H_1/V_1 peak velocities were higher during abducting saccades than adducting saccades especially at near but with high inter-trial variations. The velocities of θ_H/θ_V almost doubled while those of H_1/V_1 changed little with increasing accommodative stimulus. This implies that saccade rates are not affected by accommodative stimulus. The doubling of the θ_H/θ_V velocities is likely the result of the increase in lens instability affected by accommodative effort.

Age-related changes

Deubel and Bridgeman (1995) mainly investigated pre-presbyopes. Only two of their subjects were above 50 years old (54 and 55). Although ten subjects in the current study were full presbyopes, their ages ranged from 53 to 71 years. Onset of accommodative lens instability could theoretically occur either before or after the total loss of accommodation. Therefore, the age-related changes in artifact/saccade ratios were investigated, both in the unaccommodated and accommodated states for all subjects (Figure 9). There was no significant change in the ratio with age for either the unaccommodated [$F(1,9) = 0.04$, $p = 0.844$] or accommodated [$F(1,9) = 1.95$, $p = 0.201$] states.

Cycloplegia

A pre-presbyopic subject with 1.34 D of accommodation and a fully presbyopic subject were tested in the same
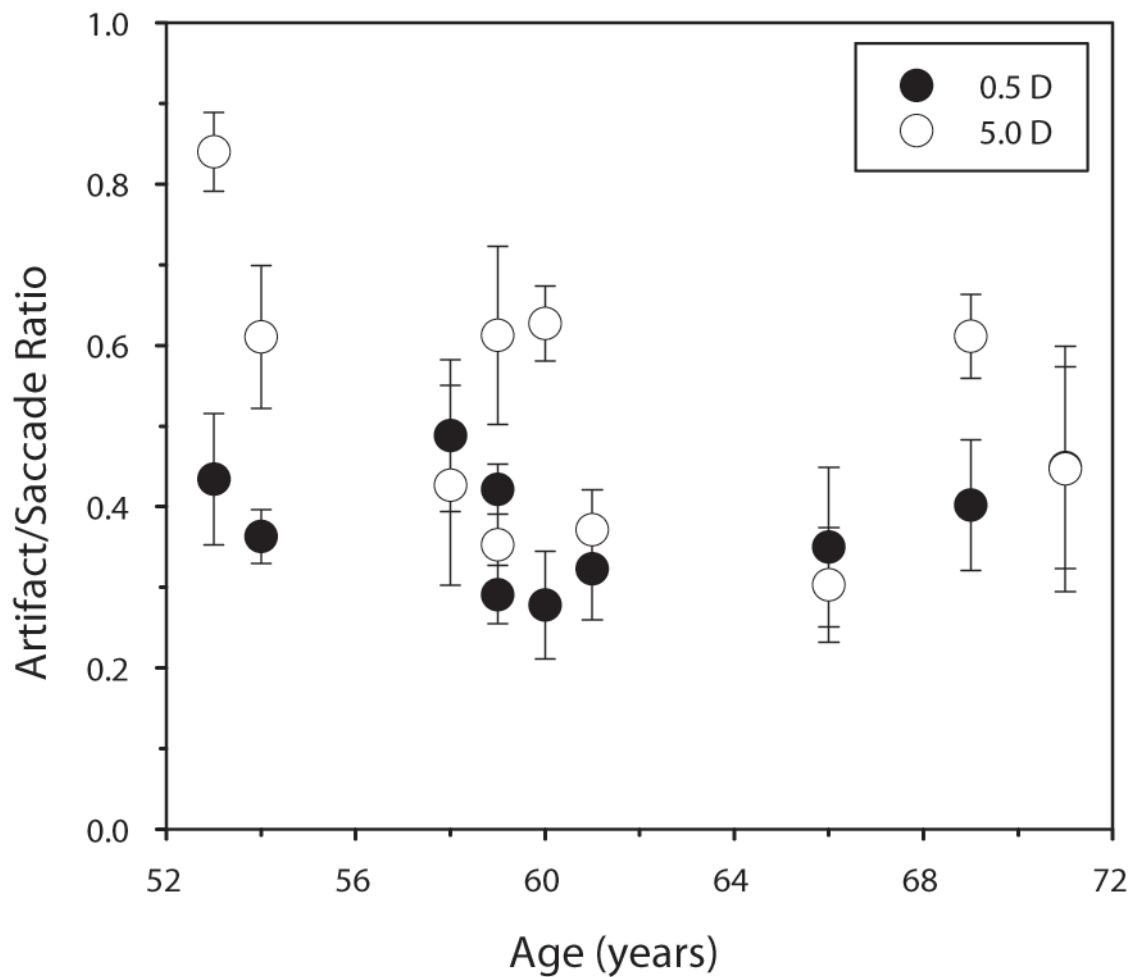
Figure 9. Age-related changes of artifact/saccade ratio. The solid circles are the artifact/saccade for a 0.5-D accommodative stimulus; the open circles are the artifact/saccade for a 5-D accommodative stimulus. Error bars are ±1 standard deviation. No systematic age-related trend is observed.

protocol with and without two drops of 1% tropicamide cycloplegia. The accommodative change in artifact/saccade ratio decreased markedly after cycloplegia in both subjects (Figure 10). The results demonstrate that paralysis of the ciliary muscle reduces accommodative lens instability during saccades.

Ray tracing

While the eye tracker can detect the lens wobble artifact, it cannot distinguish what kind of lens motion occurs during saccades to cause the lens wobble artifact. There are two possibilities, i.e., tilt (lens rotational movement) and decentration (lens translational movement). The schematic eye modeling provides an estimation of the magnitude of the lens wobble artifact caused by translating or tilting the lens (Figure 11). The calculated lens wobble artifact increases linearly with the amount of lens translation and lens tilt. To achieve a 1° lens wobble artifact amplitude, the lens must translate by 0.125 mm or tilt by 3°. Similar ray tracing methods exploring the locations of Purkinje images were introduced by Clement, Dunne, and Barnes (1987) using Kooijman's schematic eye. Their result, which showed that lens translation of 1 mm is approximately five times greater than lens tilt of 5°, is very close to that reported in the current study. Since it is unlikely that the lens would tilt more than the amount of eye rotation, i.e., 4°, a pure lens tilt of 4° during saccades would produce a lens wobble amplitude of only 1.3°. Since lens wobble artifacts of up to 4.2°
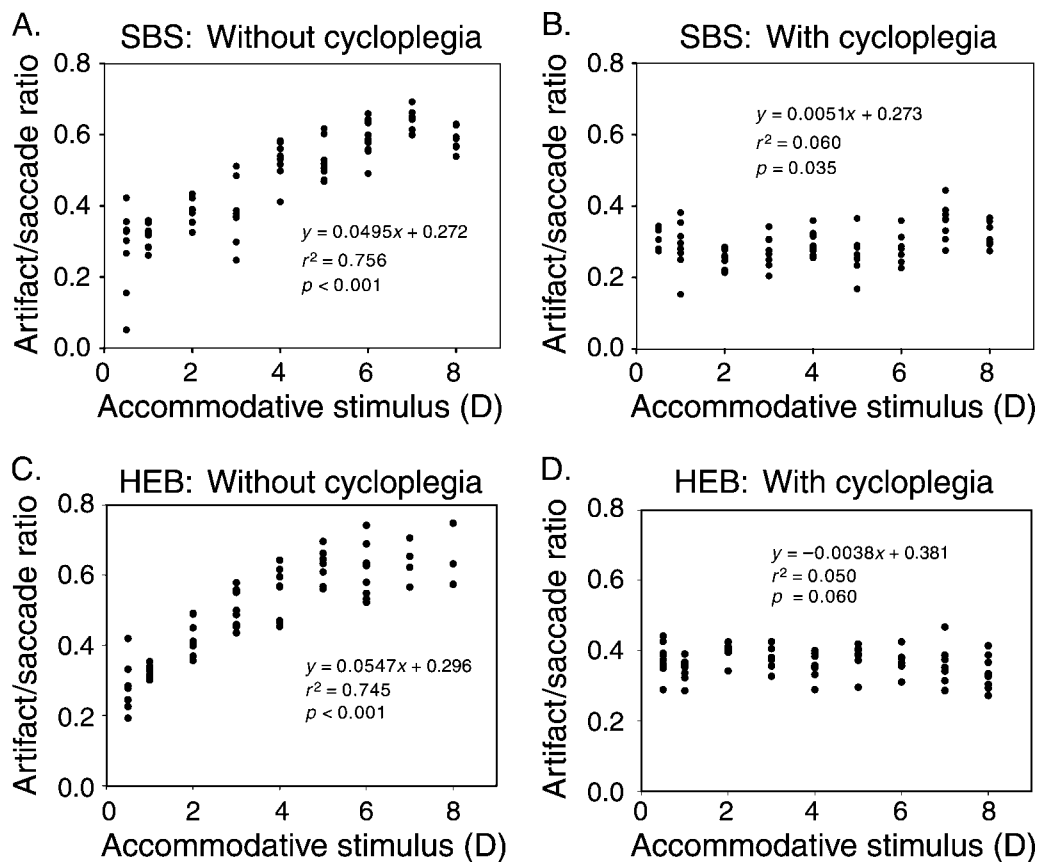
Figure 10. The artifact/saccade ratio as a function of accommodative stimulus amplitude from (A, B) a pre-presbyopic subject with 1.34 D of accommodation and (C, D) a fully presbyopic subject (A, C) before and (B, D) after 1% tropicamide cycloplegia. For both subjects, the ratios are not dependent on stimulus amplitude after cycloplegia, suggesting that accommodative contraction of the ciliary muscle releases zonular tension to allow the lens wobble to occur.

were recorded, this implies that there must be some lens translation during saccades either with or without lens tilt.

Discussion

The dPi eye tracker was used to evaluate lens wobble during saccades. In the current study, the overshoots recorded by the tracker at the end of saccades were verified to be a reliable metric for quantifying lens wobble. The eye tracker has a temporal resolution of 100 Hz. This is better than ultrasound biomicroscopy (UBM; ~10 Hz) and typical CCD cameras (~60 Hz) for high-speed dynamic measurement, especially during saccades that have relatively larger peak velocities and high frequencies. The high temporal resolution permits recording a rapid lens motion if it occurs.

Overshoot artifacts recorded at the end of saccades by the eye tracker were recognized as an undesirable artifact of eye movements and have been inferred to be lens wobble artifacts accompanying saccades (Crane & Steele, 1978; Deubel & Bridgeman, 1995; Schachar, Davila, Pierscionek, Chen, & Ward, 2007). Since the lens wobble artifacts were not consistent from saccade to saccade, Crane and Steele (1978) regarded it as unlikely that the artifacts were systematic errors from the instrumentation servomotors. They considered that the artifact reflected crystalline lens wobble. A recent study (Schultz et al., 2009) has also independently recorded lens wobble artifacts using a 1000-Hz digital video camera to capture P1 and P4. They found similar amplitudes of saccade overshoots in the P4 motion, confirming that the overshoots recorded by dual Purkinje trackers are due to lens wobble. Bahill et al. (1975a, 1975b) described overshoots that also occurred at the end of saccade. They called it "dynamic overshoot" and their existence was later verified by Kapoula et al. (1986). These studies concluded that dynamic overshoot resulted from a braking pulse at the end of a saccade and served no useful purpose. Therefore, this kind of overshoot has a saccadic or neural origin. Similarly, it is necessary to justify that the overshoots recorded by dPi eye tracker have a lens origin before using it as a tool measuring lens wobble artifact. Deubel
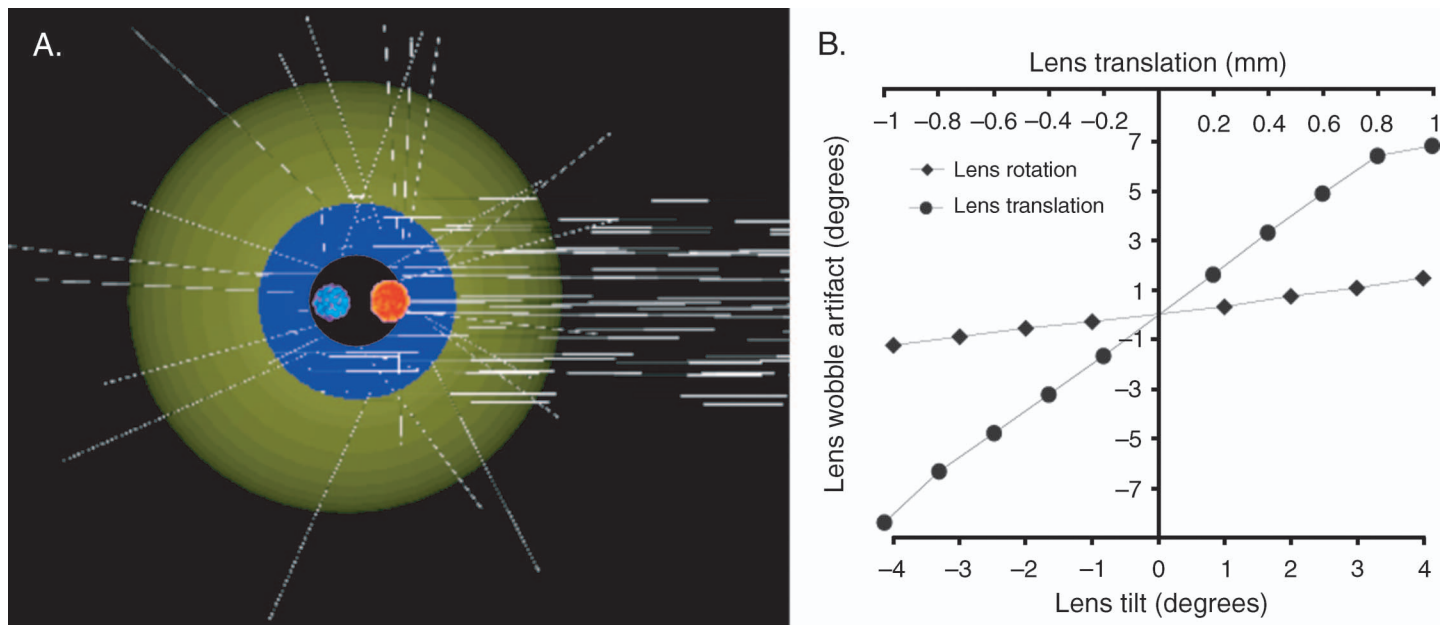
Figure 11. (A) A ray tracing eye model (Advanced Human Eye Model, AHEM, Breault Research Organization) was used to model the fourth Purkinje image shifts for a certain range of lens translations and tilts. The relative positions of the Purkinje images (red: P1; blue: P4) were identified so their movements could be measured and quantified. (B) Ray tracing analysis of movements of P1 and P4 with either lens tilt or lens translation shows the extent of lens wobble artifact in degrees. For instance, to achieve a lens wobble artifact of $\pm 1°$, the lens needs to either translate ± 0.125 mm or tilt $\pm 3°$.

and Bridgeman (1995) simultaneously used both a dPi eye tracker and magnetic search coils (Collewijn, 1977; Robinson, 1963) to measure saccades. Theoretically, subtracting the recordings from these two methods can provide pure lens motion profiles. However, one potential problem with this approach could come from different mechanic characteristics between the eye tracker and a search coil. If there is latency between these two recordings, this will produce errors. In addition, coils could slip during saccades since cyclotorsion might occur. Methodology in the current study could avoid this kind of error. Commonly, two analog channels (i.e., θ_H/θ_V channels) are used in the dPi eye tracker. These two channels include both P1 and P4 signals and are considered to represent pure eye movement. Since the isolated P4 signal is necessary to get the lens wobble effect, two other analog channels record P1 (i.e., H_1/V_1 channels). An amplitude correlation was applied to calibrate the amplitudes between the channels. The subtracted profiles therefore represent lens motion without a saccadic component. Almost all the subtracted profiles show the lens wobble artifact. Some of the artifacts were as large as the saccades. The lens wobble artifact occurrence and amplitudes recorded in the current study are much larger than 13% and 0.15° reported by Kapoula et al. (1986). Since the approach used in the current study, namely subtracting H_1/V_1 from θ_H/θ_V can still include head movement artifact, further frequency analysis was performed by comparing the profiles immediately before saccades and during saccades. The results

showed that in the older subjects who had some head tremors, the frequency of head movements was less than 5 Hz in general compared with a lens wobble frequency of around 20 Hz. Furthermore, the recordings from the eye tracker were fairly consistent with extracted traces from video clips in which the Purkinje image movements were compared directly with lens wobble as identified from the cuneiform cataract. Therefore, all these different analyses support that the artifacts arise from crystalline lens wobble.

Under the Helmholtz theory of accommodation, the lens becomes less stable during accommodation due to ciliary muscle contraction and decreased zonular tension (Glasser & Kaufman, 1999). The video clips and eye tracker recordings present both direct observations and measurement of the changes in lens suspension during accommodation and when the eye is unaccommodated. The results provide yet further evidence to support Helmholtz theory of accommodation and demonstrate that the lens is under reduced tension with greater accommodative effort in presbyopes. It is widely recognized that the lens becomes stiffer with increasing age and that this contributes to the progression of presbyopia. Studies show that the presbyopic lens is ultimately unable to undergo accommodative changes either with mechanical stretching (Glasser & Campbell, 1998) or with accommodative effort (Strenk et al., 1999). More recently, Heys et al. (2004) and Weeber et al. (2005, 2007; Weeber & van der Heijde, 2008) measured Young's modulus in different regions of

the lens. Both groups show that Young's modulus increased with age, especially in the lens nucleus. The question of whether the ciliary muscle loses its contractility with increasing age is important to understanding the etiology of presbyopia and in understanding if it may be possible to restore accommodation to the presbyopic eye with accommodative intraocular lenses. In the current study, the greater lens wobble artifact with increasing accommodative effort demonstrates that ciliary muscle still can contract even after accommodation is lost. These results are consistent with the previous MRI (Strenk et al., 1999, 2006) and UBM studies (Stachs et al., 2002), which show ciliary muscle contraction in presbyopes.

This is the first study to evaluate the ciliary muscle function with a range of accommodative stimulus amplitudes in presbyopes. Previous studies only compared the changes between unaccommodated and accommodated states (Deubel & Bridgeman, 1995; Stachs et al., 2002; Strenk et al., 1999, 2006). Although nine of ten subjects reached a statistical significance slope from the linear regression of artifact/saccade ratio to accommodative stimulus amplitude, this relationship varied across subjects (Figure 5). This variance may be due to the extent of the accommodative effort made by each individual. Although pupil constriction and convergence were also measured in this study, these cannot be used to accurately represent accommodative effort. It is expected that accommodative effort will vary between different individuals depending on their experience and familiarity with the experiments or tasks; therefore, this inter-individual variability is not unexpected.

The directional difference of the artifact amplitudes was also noticed by Deubel and Bridgeman (1995). Both studies show significantly larger wobbles following abducting saccades than adducting saccades. In the current study, the acceleration and deceleration profiles of both θ_H/θ_V and H_1/V_1 during abducting saccades have larger velocities and accelerations than during adducting saccades, especially when subjects make accommodative efforts. A prior study showed that abducting saccades have larger amplitudes, higher peak velocities, and shorter durations than adducting saccades (Collewijn et al., 1988a). The asymmetry could be attributed to an extraocular cause such as the unbalanced force of the medial and lateral rectus muscles or their unbalanced neural control during saccades. Another possible explanation is an intraocular asymmetry in the ciliary muscle contraction or zonular elasticity. The possibility is supported by MRI studies (Strenk, Strenk, & Semmlow, 2000) and UBM studies (Glasser, Croft, Brumback, & Kaufman, 2001), in which an asymmetric nasal and temporal circumlental space was observed. It is inferred that the asymmetries resulted from nasal/temporal differences in ciliary muscle dimensions, i.e., the ciliary muscle is larger on the temporal side than on the nasal side. This could be a possible explanation for the asymmetries in the lens wobble amplitudes.

Another strong indication that amplitudes of lens wobble artifacts were related to ciliary muscle function comes from applying tropicamide cycloplegia to paralyze the ciliary muscle. If the ciliary muscle cannot contract with a greater accommodative stimulus, lens instability should not increase with increasing accommodative stimulus amplitude. Both subjects show a dramatic decrease in the slope of this relationship after cycloplegia.

In the current study, the subject ages ranged from 53 to 71 years. There is no significant age-related change in lens wobble effect in these full presbyopes as shown (Figure 9). Theoretically, the lens wobble artifact during saccades could be mainly determined by the lens and ciliary body configuration. The lens factors include lens mass and lens diameter. It is well known that the wet weight of the lens increases throughout the life span (Augusteyn, 2007; Brown & Bron, 1996; Glasser & Campbell, 1999). Since lens wobble is a result of inertia, then the greater the lens mass, the larger the wobble amplitude should be. As for the lens diameter, Wendt, Croft, McDonald, Kaufman, and Glasser (2008) show in rhesus monkeys that age-related changes included decreasing ability of the lens to undergo changes in thickness and diameter with accommodation, however without an age-related change in unaccommodated lens diameter. A similar result is found in humans (Strenk et al., 1999). The influence of the ciliary body in lens wobble lies in its baseline (unaccommodated) configuration and how much the ciliary muscle can move toward the lens equator during accommodation. Tamm, Tamm, and Rohen (1992) showed that the ciliary muscle shifts progressively toward an anterior-inward configuration with increasing age. This means that the distance between the apex of the ciliary body and the lens equator (circumlental space) decreases with age. Therefore, the circumlental space that is influenced by the lens diameter and ciliary muscle configuration may be the most important factor in determining the wobble amplitude. Although it is possible that circumlental space could be a factor affecting the lens wobble amplitude among the subjects, there is no indication on how large the circumlental space was in the subjects in the current study. Furthermore, in young subjects, circumlental space and zonular tension may not decrease much with low accommodative responses because the lens diameter decreases during accommodation. Therefore, only full presbyopes were used in the current study. The lenses of presbyopes are too stiff to undergo any accommodative diameter changes. Thus the lens wobble effect, theoretically, only depends on how much the ciliary muscle contracts. This is dependent on how much accommodative efforts these presbyopes made, not on their age. The point is that the ciliary muscle still works in the presbyopic eye. Since the lens wobble artifact did not differ with age, it means all these subjects can make similar accommodative efforts. The ability to measure circumlental space with accommodative effort would also be helpful to understand ciliary muscle function with increasing age. However,

using the lens wobble artifact as a surrogate measure for ciliary muscle contraction is limited because other factors, such as the lens mass and the ciliary muscle configuration changes need to be taken into account. The complexity caused by multiple variables may contribute to individual variations observed.

The modeling helps determine what kind of lens motion is more likely to occur during saccades. Lens tilt alone cannot account for the lens wobble amplitudes recorded, which implies that there must also be lens translation occurring. In the video, recordings of the cuneiform cataract motion in that particular subject showed irregular motion, which could include both tilt and translation or could be due to an inability to track that object cleanly in the video images.

Conclusion

Since most subjects showed increasing lens instability, it is clear that the ciliary muscle still contracts and moves with accommodative effort in these subjects. The current study supports former MRI and UBM studies (Stachs et al., 2002; Strenk et al., 1999, 2006), which demonstrate ciliary muscle movements in presbyopes, but extends those findings to show that not only is ciliary muscle function preserved in presbyopes, but further is capable of greater accommodative excursions with greater accommodative efforts. Thus, it appears that ciliary muscle function is preserved in its capacity to move not only in terms of its existence but also in terms of its reserve. Preserved ciliary muscle function in presbyopes provided the possibility of restoring accommodation after implanting accommodative intraocular lenses (A-IOLs) if the IOLs are designed to function in accordance with the physiological mechanism of accommodation.

Acknowledgments

Commercial relationships: William J. Donnelly III, Breault Research Organization (E).
Corresponding author: Scott B. Stevenson.
Email: sbstevenson@uh.edu.
Address: College of Optometry, University of Houston, 4901 Calhoun Road, Houston, TX 77204, USA.

References

Augusteyn, R. C. (2007). Growth of the human eye lens. *Molecular Vision, 13,* 252–257. [PubMed] [Article]

Bahill, A. T., Clark, M. R., & Stark, L. (1975a). Computer simulation of overshoot in saccadic eye movements. *Computer Programs in Biomedicine, 4,* 230–236. [PubMed]

Bahill, A. T., Clark, M. R., & Stark, L. (1975b). Dynamic overshoot in saccadic eye movements is caused by neurological control signed reversals. *Experimental Neurology, 48,* 107–122. [PubMed]

Brown, N. P., & Bron, A. J. (1996). *Lens disorders. A clinical manual of cataract diagnosis.* Oxford, UK: Butterworth-Heinemann.

Clement, R. A., Dunne, M. C. M., & Barnes, D. A. (1987). A method for ray tracing through schematic eyes with off-axis components. *Ophthalmic & Physiological Optics, 7,* 149–152. [PubMed]

Collewijn, H. (1977). Eye- and head movements in freely moving rabbits. *The Journal of Physiology, 266,* 471–498. [PubMed] [Article]

Collewijn, H., Erkelens, C. J., & Steinman, R. M. (1988a). Binocular co-ordination of human horizontal saccadic eye movements. *The Journal of Physiology, 266,* 157–182. [PubMed] [Article]

Collewijn, H., Erkelens, C. J., & Steinman, R. M. (1988b). Binocular co-ordination of human vertical saccadic eye movements. *The Journal of Physiology, 404,* 183–197. [PubMed] [Article]

Cornsweet, T. N., & Crane, H. D. (1973). Accurate two-dimensional eye tracker using first and fourth Purkinje images. *Journal of the Optical Society of America, 63,* 921–928. [PubMed]

Crane, H. D., & Steele, C. M. (1978). Accurate 3-dimensional eye tracker. *Applied Optics, 17,* 691–705.

Crane, H. D., & Steele, C. M. (1985). Generation-V dual-Purkinje-image eye tracker. *Applied Optics, 24,* 527–537. [PubMed]

Deubel, H., & Bridgeman, B. (1995). Fourth Purkinje image signals reveal eye-lens deviations and retinal image distortions during saccades. *Vision Research, 35,* 529–538. [PubMed]

Donnelly, W., 3rd (2008). The Advanced Human Eye Model (AHEM): A personal binocular eye modeling system inclusive of refraction, diffraction, and scatter. *Journal of Refractive Surgery, 24,* 976–983. [PubMed]

Duane, A. (1912). Normal values of accommodation at all ages. *The Journal of the American Medical Association, 20,* 132–157.

Duane, A. (1922). Studies in monocular and binocular accommodation, with their clinical application. *Transactions of the American Ophthalmological Society, 20,* 132–157. [PubMed] [Article]

Fincham, E. F. (1937). The mechanism of accommodation. *British Journal of Ophthalmology, 21*(Suppl. VIII), 5–80.

Fincham, E. F. (1955). The proportion of ciliary muscular force required for accommodation. *The Journal of Physiology, 128,* 99–112. [PubMed] [Article]

Glasser, A., & Campbell, M. C. (1998). Presbyopia and the optical changes in the human crystalline lens with age. *Vision Research, 38,* 209–229. [PubMed]

Glasser, A., & Campbell, M. C. (1999). Biometric, optical and physical changes in the isolated human crystalline lens with age in relation to presbyopia. *Vision Research, 39,* 1991–2015. [PubMed]

Glasser, A., Croft, M. A., Brumback, L., & Kaufman, P. L. (2001). Ultrasound biomicroscopy of the aging rhesus monkey ciliary region. *Optometry and Vision Science, 78,* 417–424. [PubMed]

Glasser, A., & Kaufman, P. L. (1999). The mechanism of accommodation in primates. *Ophthalmology, 106,* 863–872. [PubMed]

Gullstrand, A. (1908). Die optische abbildung in heterogenen medien die dioptrik der kristallinse des menschen [reviewed in English by Eskridge, J. B. (1984). Review of ciliary muscle effort in presbyopia. *American Journal of Optometry and Physiological Optics, 61,* 133–138. [PubMed]]. *Kungl. Svenska Vetenskapsakademiens Handlingar, 43,* 1–28.

Hess, C. (1901). Arbeiten aus dem gebiete der accommodationslehre. VI: Die relative accommodation [reviewed in English by Atchison, D. A. (1995). Accommodation and presbyopia. *Ophthalmic & Physiological Optics, 15,* 255–272. [PubMed]]. *Albrecht von Graefe's Archiv für Ophthalmologie, 52,* 143–174.

Heys, K. R., Cram, S. L., & Truscott, R. J. (2004). Massive increase in the stiffness of the human lens nucleus with age: The basis for presbyopia? *Molecular Vision, 10,* 956–963. [PubMed] [Article]

Kapoula, Z. A., Robinson, D. A., & Hain, T. C. (1986). Motion of the eye immediately after a saccade. *Experimental Brain Research, 61,* 386–394. [PubMed]

Melvill Jones, G., & Gonshor, A. (1982). Oculomotor response to rapid head oscillation (0.5–5.0 Hz) after prolonged adaptation to vision reversal. "Simple" and "complex" effects. *Experimental Brain Research, 45,* 45–58. [PubMed]

Robinson, D. A. (1963). A method of measuring eye movement using a sclera search coil in field. *IEEE Transactions on Biomedical Engineering, 10,* 137–145. [PubMed]

Schachar, R. A., Davila, C., Pierscionek, B. K., Chen, W., & Ward, W. W. (2007). The effect of human in vivo accommodation on crystalline lens stability. *British Journal of Ophthalmology, 91,* 790–793. [PubMed]

Schultz, K. E., Sinnott, L. T., Mutti, D. O., & Bailey, M. D. (2009). Accommodative fluctuations, lens tension, and ciliary body thickness in children. *Optometry and Vision Science, 86,* 677–684. [PubMed]

Schwiegerling, J. (2004). *Field guide to visual and ophthalmic optics.* Bellingham, WA: SPIE Press.

Stachs, O., Martin, H., Kirchhoff, A., Stave, J., Terwee, T., & Guthoff, R. (2002). Monitoring accommodative ciliary muscle function using three-dimensional ultrasound. *Graefe's Archive for Clinical and Experimental Ophthalmology, 240,* 906–912. [PubMed]

Strenk, S. A., Semmlow, J. L., Strenk, L. M., Munoz, P., Gronlund-Jacob, J., & DeMarco, J. K. (1999). Age-related changes in human ciliary muscle and lens: A magnetic resonance imaging study. *Investigative Ophthalmology & Visual Science, 40,* 1162–1169. [PubMed] [Article]

Strenk, S. A., Strenk, L. M., & Guo, S. (2006). Magnetic resonance imaging of aging, accommodating, phakic, and pseudophakic ciliary muscle diameters. *Journal of Cataract & Refractive Surgery, 32,* 1792–1798. [PubMed]

Strenk, S. A., Strenk, L. M., & Semmlow, J. L. (2000). High resolution MRI study of circumlental space in the aging eye. *Journal of Refractive Surgery, 16,* S659–S660. [PubMed]

Tamm, S., Tamm, E., & Rohen, J. W. (1992). Age-related changes of the human ciliary muscle. A quantitative morphometric study. *Mechanisms of Ageing and Development, 62,* 209–221. [PubMed]

Weeber, H. A., Eckert, A. G., Soergel, F., Meyer, C. H., Pechhold, W., & van der Heijde, R. G. (2005). Dynamic mechanical properties of human lenses. *Experimental Eye Research, 80,* 425–434. [PubMed]

Weeber, H. A., Eckert, G., Pechhold, W., & van der Heijde, R. G. (2007). Stiffness gradient in the crystalline lens. *Graefe's Archive for Clinical and Experimental Ophthalmology, 245,* 1357–1366. [PubMed]

Weeber, H. A., & van der Heijde, R. G. (2008). Internal deformation of the human crystalline lens during accommodation. *Acta Ophthalmologica, 86,* 642–647. [PubMed]

Wendt, M., Croft, M. A., McDonald, J., Kaufman, P. L., & Glasser A. (2008). Lens diameter and thickness as a function of age and pharmacologically stimulated accommodation in rhesus monkeys. *Experimental Eye Research, 86,* 746–752. [PubMed]